JOC The Journal of Organic Chemistry

Article

pubs.acs.org/joc

Charge-Transfer Interactions in a Multichromophoric Hexaarylbenzene Containing Pyrene and Triarylamines

Christoph Lambert,* Julia Ehbets, Dirk Rausch, and Markus Steeger

Institut für Organische Chemie, Universität Würzburg, Wilhelm Conrad Röntgen Research Center for Complex Material Systems, Würzburg, Center for Nanosystems Chemistry, Am Hubland, 97074 Würzburg, Germany

Supporting Information

ABSTRACT: Two different hexaarylbenzenes with three pyrene and three triarylamine substituents in different positions (trigonal symmetric and asymmetric arrangement) were synthesized, and their charge-transfer states were investigated by optical spectroscopy. In these multichromophoric systems triarylamine acts as the electron donor and pyrene as the electron acceptor. A reference chromophore with only one donor−acceptor pair was also investigated. All these chromophores form charge-transfer states upon photoexcitation which relax with a moderate fluorescence quantum yield to the ground state. The compounds do not differ significantly concerning most of their fluorescence properties, which shows that the fluorescent charge-transfer state is very similar in all chromophores. This observation indicates symmetry breaking for the symmetric chromophore within fluorescence lifetime of several tens of ns. This interpretation was substantiated by fluorescence excitation anisotropy measurements in a sucrose octaacetate matrix.

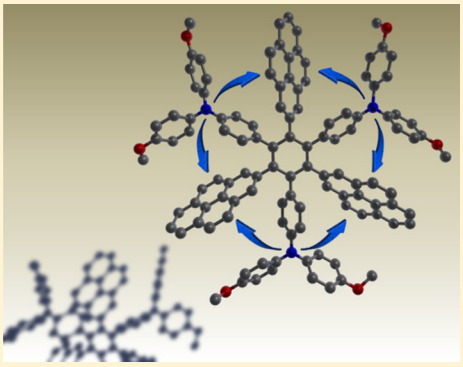

INTRODUCTION

Pyrene is a versatile chromophore that may act both as an electron donor and an electron acceptor.[1] In this paper, we combine three pyrene units with three triarylamine moieties in a hexaarylbenzene (HAB) superchromophore assembly in order to probe charge-transfer processes and energy migration within this system. The triarylamines are strong electron donors that force the pyrenes to be the acceptors.

Pyrene itself shows some unique optical properties: a long fluorescence lifetime (354 ns),[2] delayed fluorescence as a consequence of triplet−triplet annihilation, and excimer formation in concentrated solution are only the highlights.[3] Most of these properties are the consequence of a very weak $S_1 \leftarrow S_0$ transition (L_b band in Platt's terminology) at ca. 370 nm which is polarized perpendicularly to the long axis[4] and which is due to a combination of HOMO-1→LUMO and HOMO→LUMO+1 excitation (see Figure 1).[2] The most prominent absorption at 334 nm, however, shows a pronounced vibrational progression and is polarized along the long axis of pyrene. This refers to a HOMO→LUMO transition. Despite the long fluorescence lifetime, the fluorescence quantum yield of unsubstituted pyrene is relatively high (0.64 in toluene)[2] because intersystem crossing ($k_{ISC} = 10^5\ s^{-1}$) is even slower than the rate of fluorescence ($k_f = 10^6\ s^{-1}$). Owing to these facts, pyrene has recently gained much attention because its luminescent properties may be used in organic light-emitting diodes (OLEDs)[5−7] and other optoelectronic devices,[8] as well as for biolabeling.[9,10]

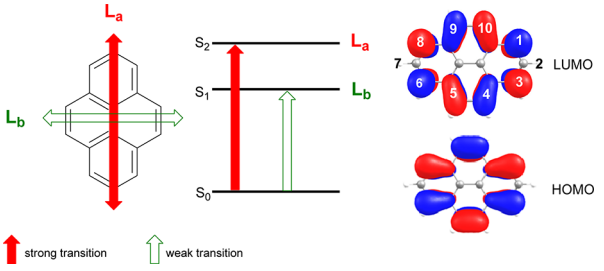

Figure 1. Optical transitions in pyrene.

Triarylamines are important hole-conducting materials for optoelectronic devices, most importantly for OLEDs but also for electrophotography.[11−16] The donor strength can easily be tuned by substituents in *ortho*- and *para*-positions whose presence is also a prerequisite for making triarylamine radical cations chemically stable as these tend to dimerize at the otherwise unblocked *para*-position.[17,18] Furthermore, the relatively small reorganization energy of the triarylamines supports fast electron-transfer processes.

Interactions between amines and pyrene have been investigated quite intensively in the past. These studies mostly refer to either fluorescence quenching by photoinduced electron transfer from the amine to the unsaturated hydrocarbon[19−25] or to charge-transfer processes in which the two redox chromophores were involved.[1,26−28] While in the former process fluorescence from the S_1 state of pyrene is quenched by the formation of pyrene radical anions, in the latter CT states

Received: May 8, 2012
Published: June 25, 2012

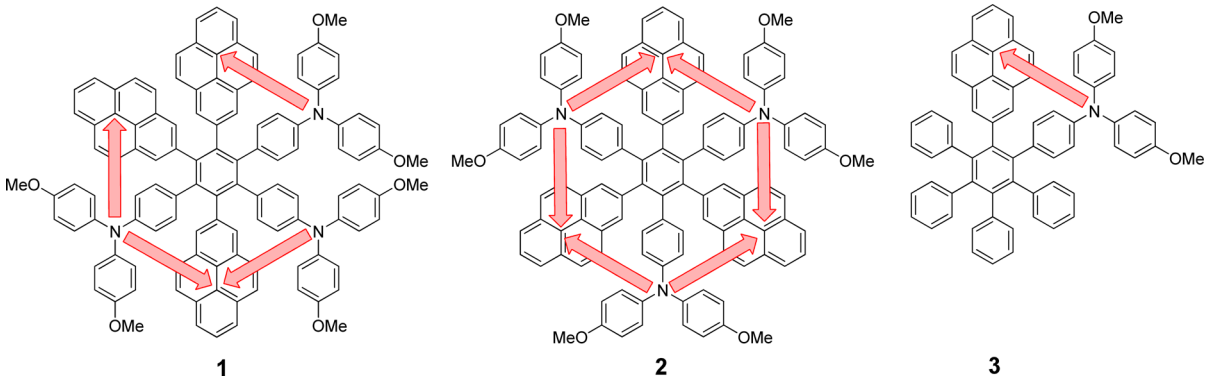

Figure 2. Charge-transfer interactions in the multidimensional chromophores **1**–**3**.

Scheme 1. Synthesis of 1–3

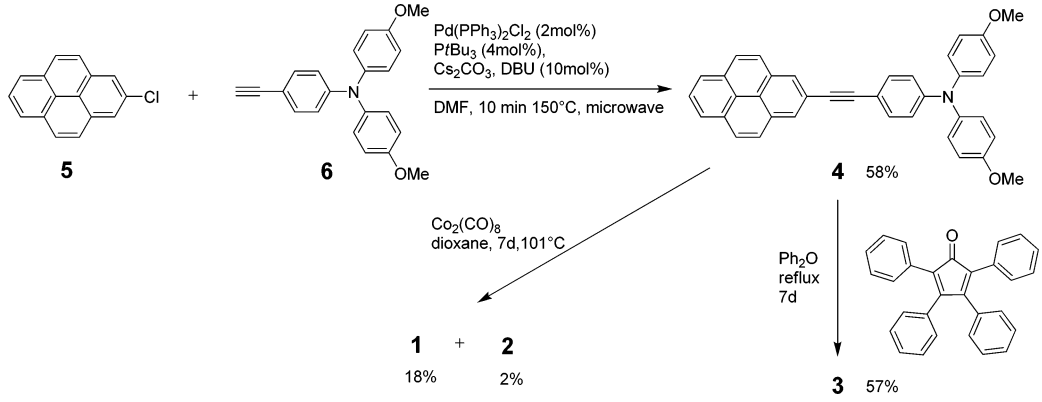

are formed from which fluorescence now occurs in a much different way than from pyrene's local S_1 state. In the majority of these works pyrene is substituted at its 1-position because of easier synthetic accessibility. However, following the work of Marder et al.,[29,30] substitution at the 2-position is readily achieved and will be used in this work.

In the study presented here, we focus on through-space charge-transfer interactions between triarylamine donors and pyrene acceptors in multidimensional chromophores. As a scaffold we use hexaarylbenzene (HAB).[31] Recently, HABs have often been used as a scaffold in complex chromophore systems in order to study energy or electron-transfer processes or interchromophore interactions in general or they have been used for light-harvesting purposes.[5,32−46] In the HABs, six phenyl rings are arranged around a central benzene ring in a propeller-like fashion. The dihedral angle between the phenyl substitutents and the benzene ring is ca. 60° which reduces direct orbital overlap and, thus, conjugational effects via the benzene core. In the chromophores **1** and **2** studied here, three triarylamines and three pyrenes are attached to the central benzene and, thus, are an integral part of the HAB. Owing to the pyrenes being attached to the central benzene at their 2-position conjugational effects are minimized by the fact that the HOMO and the LUMO of pyrene possess nodes along the long molecular axis (see Figure 1).[2] Thus, the interaction between pairs of triarylamines and pyrene is mainly through-space. In the symmetric chromophore **2** with the triarylamines in 1-, 3-, and 5-position of the central benzene ring there are six through-space interactions indicated by red arrows in Figure 2. In the asymmetric isomer **1** there are only four such interactions. For comparison we also investigated a "mono-meric" analogue **3** where only one donor−acceptor pair is present.

RESULTS AND DISCUSSION

Synthesis. The HAB chromophores **1** and **2** were synthesized by cobalt-catalyzed cyclotrimerization[47] of an appropriately substituted tolan precursor molecule **4**. The cyclotrimerization is sensitive to steric hindrance, which might explain the low yield of isomer mixture of 25%. For statistical reasons, one expects the yields of the 1,3,5-isomer **2** and the 1,2,4-isomer **1** to have a 1:3 ratio which was found in similar cases before.[33,48] Indeed, pure asymmetric compound **1** could be isolated in 18% yield from the isomer mixture by precipitation from acetone. If the residue contained only compound **2** in 7% yield, this would lead to the expected ratio of 7:8≈1:3. However, in the present case we experienced problems in isolating **2** and the residue had to be purified by HPLC on a silica gel NUCLEOSIL 120−5 phase with dichloromethane to give only 2% of pure **2**. In this context it proved critical to use dichloromethane from J. T. Baker stabilized with amylene.

The reference chromophore **3** was synthesized by a Diels−Alder reaction of tetraphenylcyclopentadienone and tolan **4** in 57% yield. The synthesis of the tolan **4** proved to be tricky. Several attempts to use either 2-bromo-, 2-OTos-, or 2-OTf-substituted pyrene in Sonogashira or Stille reactions led to 20% yield at best. Finally, the synthesis of **4** was accomplished by a Sonogashira reaction of 2-chloropyrene **5** and triarylamine alkyne **6** in a microwave oven in 58% yield. The chloro compound **5** in turn was prepared from 2-pyreneboronic acid pinacol ester **7** in 97% yield. A similar reaction using 2-

dx.doi.org/10.1021/jo300924x | J. Org. Chem. 2012, 77, 6147−6154

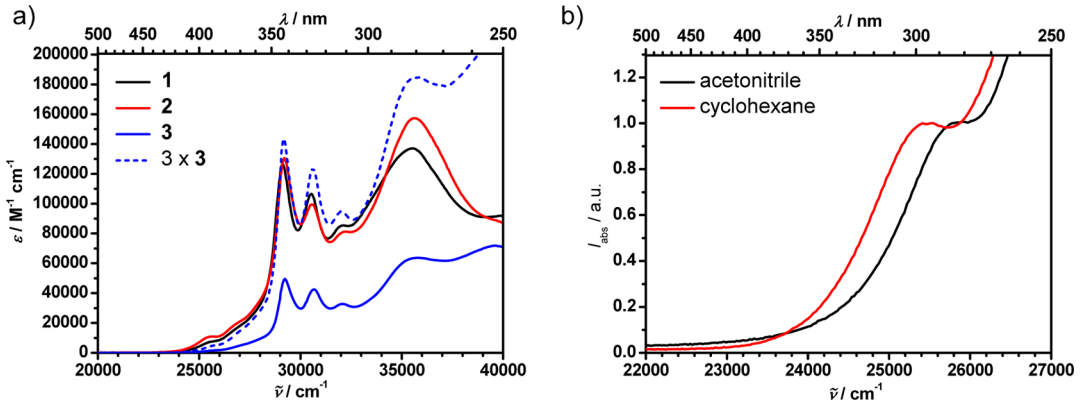

Figure 3. (a) Absorption spectra of **1**−**3** in THF; (b) magnified CT band of **2**.

iododpyrene yielded 62% of **4** but because the synthesis of 2-iodopyrene from pyrene-2-boronic acid[49] is associated with only moderate yields (30%) the route via 2-chloropyrene is preferred and presented here (Scheme 1).

UV/vis and Fluorescence Spectroscopy. The absorption spectra of **1**−**3** are very similar and show several distinct features (see Figure 3a): a broad and structureless band around 36000 cm^{-1} is mainly due to a localized $\pi-\pi^*$ excitation of the triarylamine moieties. At 29100 cm^{-1}, we identify the L_a-transition of the pyrene chromophores. This band has a pronounced vibronic progression as found in many pyrene derivatives.[4] Between 26000 and 28000 cm^{-1} there is the weak pyrene L_b band visible. Because of the localized nature of these transitions, all these bands are hardly solvatochromic. However, at ca. 25400 cm^{-1} (in cyclohexane) there is an even weaker but broad and structureless band which shows a positive solvatochromism as can be seen from the different band maximum in acetonitrile: 25800 cm^{-1} (see Figure 3b). We assign this band to a charge-transfer (CT) excitation between the triarylamine donor and the pyrene acceptor. Accordingly, this band is more intense for **2** where six CT interactions are possible than for **1** with four such interactions, while **3** shows the weakest CT band with only one interaction.

The fluorescence of **1**−**3** also shows a pronounced positive solvatochromism, e.g., the broad and featureless emission band of **3** has a maximum at 22900 cm^{-1} in cyclohexane but at 17200 cm^{-1} in acetonitrile (see Figure 4). This behavior contrasts those of unsubstituted triarylamines and of pyrene and is attributed to the CT transition between the triarylamine donor and the pyrene acceptor. Fluorescence excitation spectra are practically identical to the absorption spectra and prove the CT emission originating from the state which corresponds to the lowest energy CT absorption band at ca. 25400 cm^{-1} irrespective of the excitation energy. A plot of the reduced emission (intensity divided by $\tilde{\nu}^3$) and absorption spectra (intensity divided by $\tilde{\nu}$)[50] of **3** in cyclohexane allows us to create a mirror image of the fluorescence CT band and to identify more clearly the CT band in the absorption spectra (Figure 5). The 00-energy was determined as the intersection between both bands and is 24300 cm^{-1}.

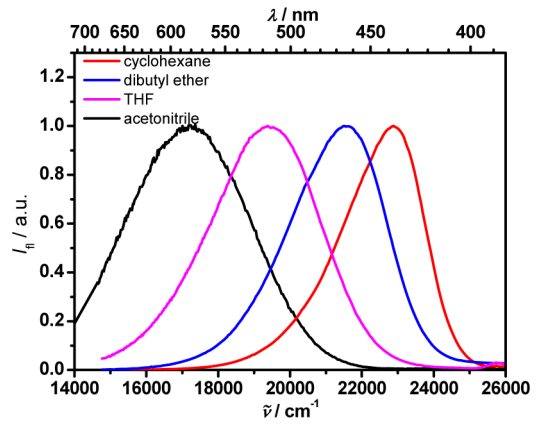

Figure 4. Fluorescence spectra of **3** in different solvents.

The fluorescence quantum yields ϕ_f of **1**−**3** were determined in different solvents (see Table 1) and do not differ significantly between the chromophores. However, the quantum yield strongly depends on the solvent polarity and ranges between ca. 7% in acetonitrile up to ca. 30% in cyclohexane. Fluorescence lifetimes of **1**−**3** were determined by a gated detection technique with pulsed LED at either 340 or 372 nm. In all cases, monoexponential decays were observed (see Figure 6) and the lifetimes were obtained by deconvolution of the decay curves with the instrument response function. The lifetimes are between ca. 45 ns in acetonitrile and ca. 25 ns in cyclohexane but again do not differ significantly for the three chromophores. With eqs 1 and 2 we calculated the rate constants for the radiative deactivation k_f and for the nonradiative deactivation k_{nr}. With k_f and the Strickler−Berg[51] eq 3 we derived the transition moments μ_{fl} which characterize the individual CT transitions. In stark contrast, it is difficult to extract the CT bands from the absorption spectra for two reasons: first, in **1** and **2** there are four and six CT transitions at similar energy, and second, the CT band overlap strongly with the L_b bands.

$$k_f = \frac{\phi_f}{\tau_f} \quad (1)$$

$$k_{nr} = \frac{1 - \phi_f}{\tau_f} \quad (2)$$

$$\mu_{fl}^2 = \frac{3h\varepsilon_0}{16\cdot 10^6 \pi^3} \cdot \frac{9}{n(n^2+2)^2} \cdot \frac{g_e}{g_g} \cdot \frac{\int \tilde{\nu}^{-3} I_f d\tilde{\nu}}{\int I_f d\tilde{\nu}} k_f \quad (3)$$

In eq 3, h is Planck's constant, ε_0 is the electric field constant, n is the index of refraction of the solvent, g_g and g_e are the degree of degeneracy of ground and excited state, and I_f is the fluorescence intensity. From Table 1 it is obvious that the transition moments are very similar for all compounds but

dx.doi.org/10.1021/jo300924x | J. Org. Chem. 2012, 77, 6147−6154

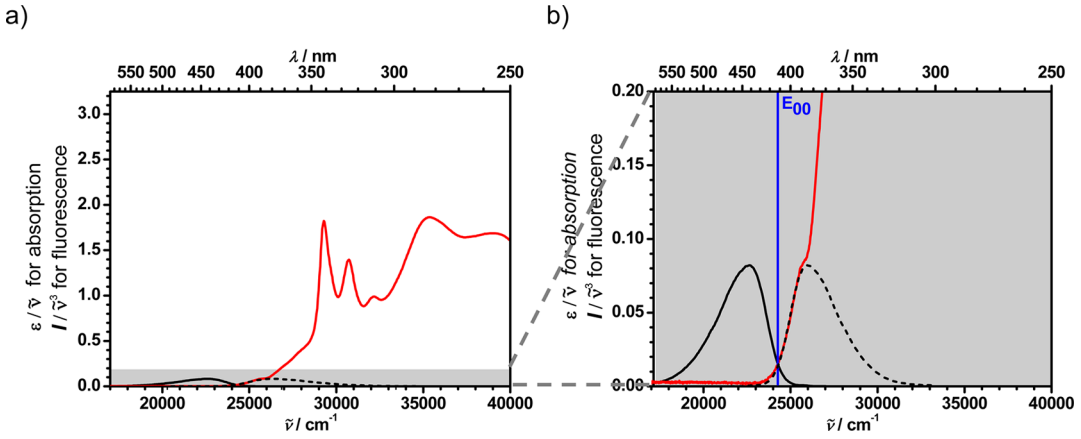

Figure 5. (a) Reduced absorption and fluorescence spectra of **3** in cyclohexane. (b) Magnification of the gray shaded area of (a).

Table 1. Fluorescence Data of 1−3[a]

		$\tilde{\nu}_{fl}$ (cm^{-1})	ϕ_f	τ_f (ns)	k_f (10^7 s^{-1})	k_{nr} (10^7 s^{-1})	μ_{fl} (D)
MeCN	1	17200	0.06	44.6[b]	0.13	2.11	0.66
	2	17200	0.07	41.9[c]	0.17	2.22	0.76
	3	17200	0.07	45.7[c]	0.15	2.02	0.71
THF	1	19300	0.15	38.3[b]	0.39	2.22	0.89
	2	19300	0.16	40.6[c]	0.39	2.07	0.89
	3	19400	0.15	40.2[c]	0.37	2.11	0.86
n-Bu_2O	1	21300	0.21	24.7[b]	0.85	3.20	1.13
	2	21300	0.24	33.9[b]	0.71	2.24	1.04
	3	21600	0.26	34.4[b]	0.76	2.15	1.06
cyclohexane	1	22600	0.22	25.6[b]	0.86	3.05	1.02
	2	22500	0.31	26.2[b]	1.18	2.63	1.20
	3	22900	0.28	30.1[b]	0.93	2.39	1.04

[a] $\tilde{\nu}_{fl}$, fluorescence energy; ϕ_f, quantum yield; τ_f, lifetime; k_f, fluorescence rate constant; k_{nr}, nonradiative rate constant; μ_{fl}, transition moment of fluorescence. [b] Excitation at 340 nm. [c] Excitation at 372 nm.

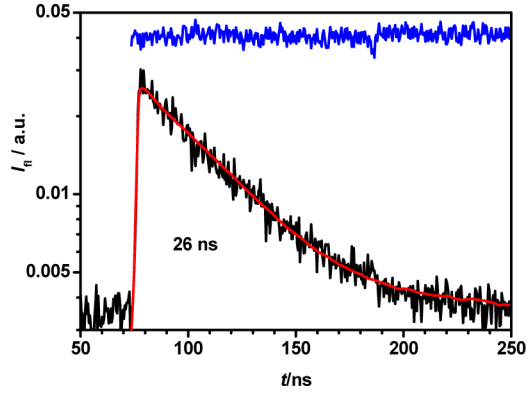

Figure 6. Fluorescence decay profile of **2** at 340 nm excitation and monoexponential fit (residues are given in blue).

increase with decreasing solvent polarity from ca. 0.7 D in acetonitrile to ca. 1.1 D in cyclohexane. The smaller transition moment in the more polar solvent is in agreement with a more complete charge transfer in acetonitrile since a 100% charge separation would require a vanishing orbital overlap between donor and acceptor and, thus, an also vanishing transition moment. The dipole moments on the order of 1 D are very similar to those recently observed in a HABs chromophore with triarylamine donors and triarylborane acceptors.[48] These HABs also show fluorescence with a similar lifetime and quantum yield. However, the fluorescence solvatochromism is much stronger in the borane based HABs than in **1**−**3** which, together with the somewhat lower CT state energy, indicates that the triarylborane is a much better electron acceptor than pyrene. However, the electronic coupling might also be stronger in the boron HABs. Both effects may enhance the dipole moment difference upon excitation and, thus, the solvatochromism.[52,53]

Fluorescence Excitation Anisotropy. In order to gain a more detailed insight into the energy-transfer processes in **1** and **2** we measured the fluorescence excitation anisotropy of these chromophores in sucrose octaacetate which forms a nonpolar solid glass matrix at rt.[54,55] Fluorescence anisotropy r is defined by eq 4 in which I_{VV} and I_{VH} is the fluorescence intensity with excitation and emission polarizer set vertically or horizontally, respectively, and G is an apparatus dependent correction factor. The anisotropy r can be related to the angle Θ of absorption and emission transition moment. Depending on this angle, r can vary between 0.4 ($\Theta = 0°$) and −0.2 ($\Theta = 90°$).[56−58]

$$r = \frac{I_{VV} - I_{VH} \cdot G}{I_{VV} + 2 \cdot I_{VH} \cdot G} = \frac{2}{5} \cdot \frac{3\cos^2 \Theta - 1}{2} \quad (4)$$

The excitation anisotropy spectra of **1**−**3** are given in Figure 8. The reference compound **3** shows anisotropy of almost 0.4 at the low energy foot of the CT absorption band. Thus, emission and absorption transition moments are almost parallel, that is, excitation is into the state from which also emission occurs. Deviations from the ideal r = 0.4 may be observed because of partial energy transfer between different molecules or because of molecular rearrangement during the excited state lifetime. At higher energy r decreases to 0.3 at 25000 cm^{-1} which is due to increasing overlap with the L_b band. At the energy of the L_b band (26000−28000 cm^{-1}) the anisotropy is around 0.2 which indicates an angle between the L_b transition moment and the CT transition of ca. 35 ± 5°. From this angle, we derive a dihedral twisting angle of the pyrene chromophore and the central benzene ring of ca. 32°. However, we stress that this angle value is associated with a very large error. At the energies of the L_a band the anisotropy drops further to ca. r = 0 and follows nicely the vibronic progression of this band. This anisotropy corresponds to a ca. 55 ± 5° angle between the transition moments of the CT and the L_a band. If we assume the CT proceeding from the center of the triarylamine to the

dx.doi.org/10.1021/jo300924x | J. Org. Chem. 2012, 77, 6147−6154

center of the pyrene we may indeed derive an angle of ca. 60° between this CT transition moment and the L_a transition moment which is polarized along the pyrene long axis. Strong overlap of higher energy pyrene bands with those of the triarylamine precludes further interpretation of the anisotropy above 33000 cm^{-1}.

The anisotropies of **1** and **2** are very similar. They start at somewhat lower values than in **3** but decrease steadily and much stronger than in **3** down to r = 0.1 at ca. 25000 cm^{-1}. Such a "red-edge excitation effect"[59−62] has frequently been observed in multidimensional chromophores and is caused by energy transfer between different states of slightly different energy within one chromophore molecule: in symmetric chromophores like **2** exciton coupling theory[63] tells us that the six equivalent CT states (see Figure 2) interact and produce a set of two pairs of degenerate CT states and two totally symmetric CT states.[64] Because of the small transition moment of the CT states (on the order of 1 D), these energy splittings will be rather small. However, even in such seemingly symmetric chromophores symmetry breaking may be induced by an asymmetric matrix (or solvent) environment which lifts the degeneracy of the CT states and leads to slightly different energies; see Figure 7.[65] If the higher energy states are excited

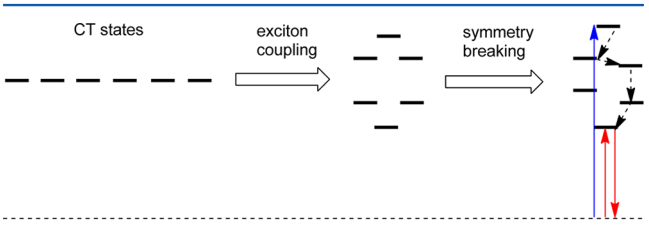

Figure 7. Six degenerate charge-transfer states in **2** couple to yield two sets of degenerate CT states and two nondegenerate CT states (within hexagonal symmetry). Symmetry breaking lifts the degeneracy. Blue arrow: excitation into higher lying states. Dashed arrows: energy transfer. Red arrows: absorption and emission into and from the lowest energy CT state.

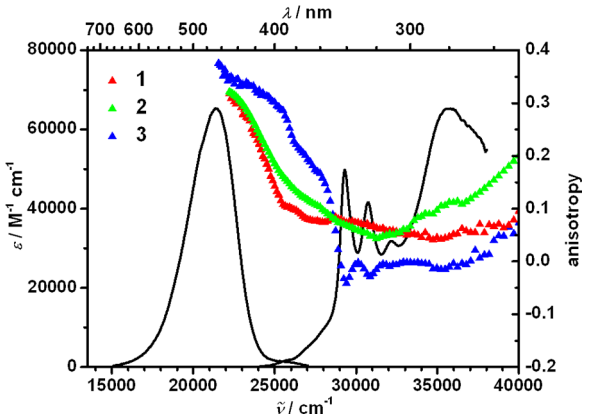

Figure 8. Fluorescence excitation anisotropy in sucrose octaacetate at rt (red, green and blue triangles). The absorption and fluorescence spectra are those of **3** in dibutyl ether.

(blue arrow in Figure 7), energy transfer between these states leads to the population of the lowest energy state from which emission occurs. This process causes a depolarization if the energy transfer is faster than the fluorescence lifetime which is a reasonable assumption given the long lifetime on the order of 10−30 ns. A total depolarization within two dimensions results in an anisotropy of r = 0.1[56,57] as indeed observed in the energy region of the L_b and L_a bands between 25000 and 33000 cm^{-1}. However one must be cautious with this interpretation because such a depolarization can also be caused accidentally by band overlap. Excitation at the red edge of the CT band (red arrow in Figure 7) populates the lowest energy state only from which emission with maximal anisotropy ($r \rightarrow 0.4$) is expected because the transition moments between excitation and emission are parallel ($\Theta = 0°$): a "red-edge excitation effect" results.

CONCLUSIONS

Sonogashira reaction of the now readily available 2-chloropyrene with ethynyltriarylamine allowed the synthesis of tolan derivatives with pyrene attached at the 2-position. Cobalt-catalyzed trimerization of these tolans led to two different HAB chromophores which form CT states upon photoexcitation. This means that in combination with triarylamine donors pyrene acts as the electron acceptor. These CT states relax with moderate fluorescence quantum yields to the ground state. The compounds **1**−**3** do not differ significantly concerning most of their fluorescence properties which indicates that the fluorescent CT state is very similar in all chromophores. For the superficially symmetric HAB **2**, this requires symmetry breaking within the fluorescence lifetime of several tens of ns, that is, after photon absorption the excitation may travel around all donor−acceptor pairs but finally gets trapped within fluorescence lifetime in one donor−acceptor pair from which emission then occurs. Because of the "round-trip"[66] through all donor−acceptor pairs depolarization with r = 0.1 within two dimensions is found at higher energies. At the lowest energy of the CT band (red edge) only those donor−acceptor pairs whose matrix surrounding and conformational orientation are energetically optimal are excited. These states fluoresce preferentially with high anisotropy ($r \rightarrow 0.4$) because energy transfer to higher lying CT states is unfavorable. The asymmetric HAB **1** is very similar to **2** in all optical characteristics which supports the above made conclusions. Model chromophore **3** shows a somewhat more detailed anisotropy which allows deducing the relative orientation of the pyrene moiety.

EXPERIMENTAL SECTION

UV/vis/NIR spectra were measured in 1 cm quartz cuvettes with a JASCO V-670 spectrometer using Uvasol solvents from Merck. Absorption spectra were recorded at ca. 1 × 10^{-5} M.

Fluorescence measurements were performed with a Photon Technology International (PTI) QM fluorescence spectrometer. Standard 1 cm cuvettes were used and spectra were recorded in Uvasol solvents from Merck after purging the samples for 15 min with argon gas. As a fluorescence standard, quinine sulfate in 1 M sulfuric acid (ϕ_f = 0.546) was used and the following equation was applied to determine the quantum yields:[67]

$$\phi_f = \phi_{f,ref}\left(\frac{I(\tilde{\nu})\cdot OD_{ref}\cdot(n_D^{20})^2}{I(\tilde{\nu})_{ref}\cdot OD\cdot(n_D^{20})^2_{ref}}\right)$$

where ϕ_f is the quantum yield of the sample, $I(\tilde{\nu})$ the integrated emission band, OD the optical density of the absorption band at the excitation wavelength, and n_D^{20} is the refraction index of the solvent.

Fluorescence lifetimes were measured with a PTI TM fluorescence lifetime spectrometer with either a pulsed 340 nm or a 372 nm LED for excitation. Colloidal silica in deionized water was used as scatter solution to determine the instrument response. Lifetimes were determined by fitting the decay curves with an exponential decay

dx.doi.org/10.1021/jo300924x | J. Org. Chem. 2012, 77, 6147−6154

function. Solvents and cuvette were used as in the steady state fluorescence experiments.

Fluorescence Excitation Anisotropy. These measurements were done with the PTI fluorescence spectrometer described above. For polarized excitation and detection, two Glan−Thompson polarizers were used. The emission was detected at 21200 cm^{-1}. For the measurements at rt sucrose octaacetate (SOA) was used as the solid matrix.[55] SOA was purchased from a commercial supplier and recrystallized from ethanol. SOA and the analyte were dissolved in dichloromethane (Uvasol) and filtered through a PTFE-filter (0.2 μm pore size). After purging with argon for 10 min, the solution was concentrated in vacuo and a colorless oil was obtained. This oil was filled in a 1 cm quartz cuvette and kept at 100 °C for 1 h and at 150 °C for 4 h in an oven in order to remove excess solvent.

Synthesis. All reagents were commercially available in standard quality and used as received. Solvents were purified according to standard procedures. Reactions requiring inert-gas conditions were carried out in flame-dried Schlenk vessels. Silica gel (40−63 μm) was obtained from a commercial supplier. Purity of the synthesized compounds was checked by inspection of the ^{13}C NMR spectra. Microwave reactions were performed in MLS μCHEMIST microwave oven using a closed pressure vessel.

2-Chloropyrene 5. Similar to ref 68. 2-Pyreneboronic acid pinacole ester (43.0 mg, 131 μmol) was dissolved in MeOH (2 mL), and a solution of $CuCl_2$ (53.0 mg, 393 μmol) in H_2O (2 mL) was added. The green mixture was stirred at 65 °C for 6 h and extracted with Et_2O (3 × 5 mL). The organic phases were washed with brine (3 × 15 mL) and dried over Na_2SO_4.The solvent was removed in vacuo, and the residue was purified by flash chromatography on silica gel with petroleum ether: yield 30.0 mg (97%) of a colorless solid; $C_{16}H_9Cl$ [236.69]; mp 136−145 °C (DCM/PE); ^1H NMR (600.1 MHz, chloroform-*d*, δ) 8.20 (d, 2 H, H-7), 8.12 (s, 2 H, H-2), 8.10 (d, 2 H, H-4), 8.03 (t, 3 H, H-8) 7.97 (d, 2 H, H-5); ^{13}C NMR (151 MHz, chloroform-*d*, δ) 132.4 (C_q), 131.8 (C_q), 130.8 (C_q), 128.6 (CH), 126.3 (CH), 126.1 (CH), 125.7 (CH), 124.23 (C_q), 124.17 (CH), 123.0 (CH).

***N,N*-Di(4-methoxyphenyl)-*N*-[4-[2-(pyrenyl)ethynyl]phenyl]-amine 4.** Alkyne **6**[69] (127 mg, 384 μmol), 2-chloropyrene **5** (91.0 mg, 384 μmol), Cs_2CO_3 (125 mg, 384 μmol), and $Pd(PPh_3)_2Cl_2$ (5.40 mg, 7.69 μmol) were dissolved in DMF (10 mL) and purged with nitrogen for ca. 5 min. After the addition of DBU (5.79 μL, 38.0 μmol) and $PtBu_3$ (1 M in toluene, 15.0 μL, 15.0 μmol), the mixture was heated at 150 °C in a microwave oven for 10 min. After being cooled to rt, ethyl acetate (10 mL) was added and the mixture was filtered over Celite and then washed with brine. The aqueous phase was extracted with ethyl acetate (3 × 5 mL), and the combined organic phases were dried over Na_2SO_4. The solvent was removed in vacuo, and the residue was purified by flash chromatography on silica gel (petroleum ether/ethyl acetate 9:1): yield 118 mg (58%) of a yellow solid; $C_{38}H_{27}NO_2$ [529.62]; mp 180-184 °C (hexane); ^1H NMR (600.1 MHz, acetone-d_6, δ) 8.38 (s, 2 H, H-2), 8.30 (d, 2 H, H-7), 8.21 (d, 2 H, H-4 o. H-5), 8.17 (d, 2 H, H-4 o. H-5), 8.08 (m, 1 H, H-8), 7.45 (AA′, 2 H, H-14 o. H-15), 7.15 (AA′, 4 H, MeO-Ph-), 6.97 (BB′, 4 H, MeO-Ph-), 6.84 (BB′, 2 H, H-14 o. H-15), 3.82 (s, 6 H, H-21); ^{13}C NMR (151 MHz, acetone-d_6, δ) 157.9 (C_q), 150.3 (C_q), 140.7 (C_q), 133.3 (CH), 132.2 (C_q), 132.1 (C_q), 129.1 (CH), 128.5 (CH), 128.1 (CH), 127.8 (CH), 127.4 (CH), 126.4 (CH), 125.0 (C_q), 124.6 (C_q), 122.4 (C_q), 119.0 (CH), 115.8 (CH), 114.0 (C_q), 91.5 (C_q), 89.2 (C_q), 55.7 (CH_3); ESI-MS pos (high resolution) *m/z* calcd for $C_{38}H_{27}NO_2$ 529.20363, found 529.20371, Δ = 0.15 ppm.

1,2,4-(Pyrenyl)-3,4,6-(4-(bis-*N,N*-(4-methoxy)phenyl)-anilino)benzene 1 and 1,3,5-(Pyrenyl)-2,4,6-(4-(bis-*N,N*-(4-methoxy)phenyl)anilino)benzene 2. Compound **4** (280 mg, 529 μmol) was dissolved in 1,4-dioxane (12 mL) under inert-gas atmosphere, and $Co_2(CO)_8$ (27.0 mg, 79.0 μmol) was added. The reaction mixture was refluxed for 7 d. The solvent was removed in vacuo, and the residue was purified by flash chromatography on silica gel (petroleum ether/dichloromethane 2:3) to give crude product as an isomer mixture. The asymmetric isomer **1** was obtained by precipitation from a concentrated solution in acetone. The residue was purified by HPLC (VP 250/10 NUCLEOSIL 120-5) in DCM to yield the symmetric isomer **2**.

Asymmetric isomer **1**: yield 150 mg (18%) of a colorless solid; $C_{114}H_{81}N_3O_6$ [1588.88]; mp 318−322 °C (DCM-d_2); ^1H NMR (600.1 MHz, dichloromethane-d_2, δ) 8.22 (d, 2 H), 8.09−8.00 (−, 7 H), 7.96−7.85 (−, 14 H), 7.77−7.71 (−, 4 H), 6.86 (AA′, 2 H), 6.79 (AA′, 2 H), 6.74 (AA′, 2 H), 6.53 (AA′, 4 H, MeO-Ph-), 6.45 (AA′, 4 H, MeO-Ph-), 6.42−6.38 (−, 6 H), 6.34 (BB′, 2 H), 6.32 (BB′, 4 H, MeO-Ph-), 6.17 (AA′, 4 H, MeO-Ph-), 6.11 (BB′, 2 H), 6.08 (BB′, 4 H, MeO-Ph-), 3.58 (s, 6 H), 3.55 (s, 6 H), 3.44 (s, 6 H); ^{13}C NMR (151 MHz, dichloromethane-d_2, δ) 155.4 (C_q), 155.3 (C_q), 155.0 (C_q), 146.4 (C_q), 146.3 (C_q), 146.2 (C_q), 141.9 (C_q), 141.8 (C_q), 141.47 (C_q), 141.46 (C_q), 141.40 (C_q), 141.35 (C_q), 141.32 (C_q), 141.2 (C_q), 140.8 (C_q), 139.5 (C_q), 139.4 (C_q), 139.2 (C_q), 134.6 (C_q), 134.5 (C_q), 134.4 (C_q), 132.7 (CH), 132.6 (CH), 132.5 (CH), 131.6 (C_q), 131.37 (C_q), 131.34 (C_q), 130.14 (C_q), 130.09 (C_q), 130.08 (C_q), 129.4 (CH), 129.3 (CH), 129.2 (CH), 127.9 (CH), 127.65 (CH), 127.59 (CH), 127.2 (CH), 127.15 (CH), 127.12 (CH), 126.0 (CH), 125.92 (CH), 125.89 (CH), 125.4 (CH), 125.3 (CH), 125.0 (CH), 124.95 (CH), 124.92 (CH), 124.89 (C_q), 124.87 (CH), 124.63 (C_q), 124.60 (C_q), 122.7 (C_q), 122.59 (C_q), 122.57 (C_q), 121.7 (CH), 121.4 (CH), 121.3 (CH), 114.43 (CH), 114.37 (CH), 114.1 (CH), 55.59 (CH_3), 55.58 (CH_3), 55.5 (CH_3); ESI-MS pos (high resolution) *m/z* calcd for $C_{114}H_{81}N_3O_6$ 1587.61199, found 1587.61302, Δ = 0.65 ppm.

Symmetric isomer **2**: yield 17.0 mg (2%) of a colorless solid; $C_{114}H_{81}N_3O_6$ [1588.88]; mp >350 °C (DCM); ^1H NMR (600.1 MHz, acetone-d_6, δ) 8.31 (d, 6 H, H-7), 8.15 (d, 6 H, H-4), 8.07 (m, 3 H, H-8), 8.00 (s, 6 H, H-2), 7.93 (d, 6 H, H-5), 6.87 (AA′, 6 H, H-15), 6.25−6.15 (−, 30 H, H-14 and MeO-Ph-), 3.47 (s, 18 H, H-21); ^{13}C NMR (151 MHz, acetone-d_6, δ) 155.8 (C_q), 147.0 (C_q), 142.4 (C_q), 141.74 (C_q), 141.70 (C_q), 140.0 (C_q), 135.3 (C_q), 133.4 (CH), 132.2 (C_q), 130.8 (C_q), 130 (CH), 128.4 (CH), 127.9 (CH), 126.8 (CH), 125.8 (CH), 125.42 (C_q), 125.37 (CH), 123.3 (C_q), 122.3 (CH), 114.8 (CH), 55.4 (CH_3); ESI-MS pos (high resolution) *m/z* calcd for $C_{114}H_{81}N_3O_6$ 1587.61199, found 1587.61318, Δ = 0.75 ppm.

1-(Pyrenyl)-2-(4-(bis-*N,N*-(4-methoxy)phenyl)amine)-3,4,5,6-(tetraphenyl)benzene 3. Compound **4** (87.0 mg, 164 μmol) and 2,3,4,5-tetraphenylcyclopenta-2,4-dienone (95.0 mg, 246 μmol) were dissolved in Ph_2O (15 mL) under inert-gas atmosphere. The mixture was refluxed for 7 d, the solvent was removed in vacuo, and the residue was purified by flash chromatography on silica gel (petroleum ether/dichloromethane 2:3): yield 83 mg (57%) of a colorless solid; $C_{66}H_{47}NO_2$ [886.09]; mp 301−304 °C (DCM/PE); ^1H NMR (600.1 MHz, dichloromethane-d_2, δ) 8.14 (d, 2 H, H-7), 7.99−7.95 (-, 3 H, H-4, H-8), 7.78 (d, 2 H, H-5), 7.71 (s, 2 H, H-2), 6.99−6.85 (m, 17 H, phenyl), 6.78−6.74 (−, 2 H, phenyl), 6.71−6.67 (−, 1 H, phenyl), 6.62 (AA′, 2 H, H-15), 6.33 (AA′, 4 H, MeO-Ph-), 6.28 (BB′, 4 H, MeO-Ph-), 6.19 (BB′, 2 H, H-14), 3.55 (s, 6 H, H-21); ^{13}C NMR (151 MHz, dichloromethane-d_2, δ) 155.4 (C_q), 146.2 (C_q), 141.5 (C_q), 141.4 (C_q), 141.20 (C_q), 141.19 (C_q), 141.15 (C_q), 141.09 (C_q), 141.08 (C_q), 140.8 (C_q), 140.74 (C_q), 140.68 (C_q), 140.6 (C_q), 139.4 (C_q), 134.3 (C_q) 132.4 (CH), 131.9 (CH), 131.82 (CH), 131.80 (2 × CH), 131.5 (C_q), 130(C_q), 129 (CH), 127.7 (CH), 127.2 (CH), 126.98 (CH), 126.94 (CH), 126.92 (2 × CH), 126.0 (CH), 125.64 (CH), 125.61 (CH), 125.59 (CH), 125.3 (2 × CH), 125.1 (CH), 124.8 (C_q), 122.5 (C_q), 121.1 (CH), 114.3 (2 × CH), 55.6 (CH_3) (4 × CH-signals of phenyl rings overlap which can be seen by integration of the appropriate signals); ESI-MS pos. (high resolution) *m/z* calcd for $C_{66}H_{47}NO_2$ 885.36013, found 885.36059, Δ = 0.52 ppm.

■ ASSOCIATED CONTENT

Supporting Information

^1H and ^{13}C NMR and mass spectra. This material is available free of charge via the Internet at http://pubs.acs.org.

■ AUTHOR INFORMATION

Corresponding Author

*E-mail: christoph.lambert@uni-wuerzburg.de.

Notes

The authors declare no competing financial interest.

■ ACKNOWLEDGMENTS

This work was supported by the Deutsche Forschungsgemeinschaft (La 991/13-1). We acknowledge the assistance of M. Moos for help with the NMR spectra and the mathematical evaluation of polarization anisotropy data.

■ REFERENCES

(1) Yang, S. W.; Elangovan, A.; Hwang, K. C.; Ho, T. I. *J. Phys. Chem. B* **2005**, *109*, 16628−16635.
(2) Crawford, A. G.; Dwyer, A. D.; Liu, Z.; Steffen, A.; Beeby, A.; Palsson, L.-O.; Tozer, D. J.; Marder, T. B. *J. Am. Chem. Soc.* **2011**, *133*, 13349−13362.
(3) Birks, J. B. *Photophysics of Aromatic Molecules*; Wiley-Interscience: London, 1970.
(4) Vasak, M.; Whipple, M. R.; Berg, A.; Michl, J. *J. Am. Chem. Soc.* **1978**, *100*, 6872−6877.
(5) Thomas, K. R. J.; Velusamy, M.; Lin, J. T.; Chuen, C. H.; Tao, Y. T. *J. Mater. Chem.* **2005**, *15*, 4453−4459.
(6) Qin, T.; Wiedemair, W.; Nau, S.; Trattnig, R.; Sax, S.; Winkler, S.; Vollmer, A.; Koch, N.; Baumgarten, M.; List, E. J. W.; Müllen, K. *J. Am. Chem. Soc.* **2011**, *133*, 1301−1303.
(7) Lai, S.-L.; Tong, Q.-X.; Chan, M.-Y.; Ng, T.-W.; Lo, M.-F.; Lee, S.-T.; Lee, C.-S. *J. Mater. Chem.* **2011**, *21*, 1206−1211.
(8) Figueira-Duarte, T. M.; Müllen, K. *Chem. Rev.* **2011**, *111*, 7260−7314.
(9) Jablonski, A. E.; Kawakami, T.; Ting, A. Y.; Payne, C. K. *J. Phys. Chem. Lett.* **2010**, *1*, 1312−1315.
(10) Sugahara, D.; Amano, J.; Irimura, T. *Anal. Sci.* **2003**, *19*, 167−169.
(11) Weiss, D. S.; Cowdery, J. R.; Young, R. H., Electrophotography. In *Electron Transfer in Chemistry*; Balzani, V., Ed.; Wiley-VCH: Weinheim, 2001; Vol. *5*, pp 379−471.
(12) Bushby, R.-J. Triarylmethyl and amine radicals. In *Magnetism: Molecules to Materials II*; Miller, J. S., Drillon, M., Eds.; Wiley-VCH: Weinheim, 2001; pp 149−187.
(13) Shirota, Y.; Kageyama, H. *Chem. Rev.* **2007**, *107*, 953−1010.
(14) Thelakkat, M. *Macromol. Mater. Eng.* **2002**, *287*, 442−461.
(15) Ning, Z.; Tian, H. *Chem. Commun.* **2009**, 5483−5495.
(16) Yen, H.-J.; Liou, G.-S. *Polym. Chem.* **2012**, *3*, 255−264.
(17) Dapperheld, S.; Steckhan, E.; Brinkhaus, K.-H. G.; Esch, T. *Chem. Ber.* **1991**, *124*, 2557−2567.
(18) Amthor, S.; Noller, B.; Lambert, C. *Chem. Phys.* **2005**, *316*, 141−152.
(19) Okada, T.; Karaki, I.; Mataga, N. *J. Am. Chem. Soc.* **1982**, *104*, 7191−7195.
(20) Mataga, N. *J. Mol. Struct.: THEOCHEM* **1986**, *135*, 279−297.
(21) Dossot, M.; Allonas, X.; Jacques, P. *Phys. Chem. Chem. Phys.* **2002**, *4*, 2989−2993.
(22) Inada, T. N.; Kikuchi, K.; Takahashi, Y.; Ikeda, H.; Miyashi, T. *J. Photochem. Photobiol., A* **2000**, *137*, 93−97.
(23) Siegmund, K.; Daublain, P.; Wang, Q.; Trifonov, A.; Fiebig, T.; Lewis, F. D. *J. Phys. Chem. B* **2009**, *113*, 16276−16284.
(24) Lewis, F. D.; Daublain, P.; Delos Santos, G. B.; Liu, W. Z.; Asatryan, A. M.; Markarian, S. A.; Fiebig, T.; Raytchev, M.; Wang, Q. A. *J. Am. Chem. Soc.* **2006**, *128*, 4792−4801.
(25) Zeidan, T. A.; Wang, Q.; Fiebig, T.; Lewis, F. D. *J. Am. Chem. Soc.* **2007**, *129*, 9848−9849.
(26) Wiessner, A.; Huttmann, G.; Kuhnle, W.; Staerk, H. *J. Phys. Chem.* **1995**, *99*, 14923−14930.
(27) Techert, S.; Schmatz, S.; Wiessner, A.; Staerk, H. *J. Phys. Chem. A* **2000**, *104*, 5700−5710.
(28) Weller, A. *Z. Phys. Chem.* **1982**, *130*, 129−138.
(29) Coventry, D. N.; Batsanov, A. S.; Goeta, A. E.; Howard, J. A. K.; Marder, T. B.; Perutz, R. N. *Chem. Commun.* **2005**, 2172−2174.
(30) Crawford, A. G.; Liu, Z.; Mkhalid, I. A. I.; Thibault, M.-H.; Schwarz, N.; Alcaraz, G.; Steffen, A.; Collings, J. C.; Batsanov, A. S.; Howard, J. A. K.; Marder, T. B. *Chem.—Eur. J.* **2012**, *18*, 5022−5035.
(31) Lambert, C. *Angew. Chem., Int. Ed.* **2005**, *44*, 7337−7339.
(32) Rathore, R.; Burns, C. L.; Deselnicu, M. I. *Org. Lett.* **2001**, *3*, 2887−2890.
(33) Lambert, C.; Nöll, G. *Chem.—Eur. J.* **2002**, *8*, 3467−3477.
(34) Sun, D.; Rosokha, S. V.; Kochi, J. K. *Angew. Chem., Int. Ed.* **2005**, 5133−5136.
(35) Rathore, R. B.; Carrie, L.; Abdelwahed, S. A. *Org. Lett.* **2004**, *6*, 1689−1692.
(36) Traber, B.; Wolff, J. J.; Rominger, F.; Oeser, T.; Gleiter, R.; Goebel, M.; Wortmann, R. *Chem.—Eur. J.* **2004**, *10*, 1227−1238.
(37) Rosokha, S. V.; Neretin, I. S.; Sun, D. L.; Kochi, J. K. *J. Am. Chem. Soc.* **2006**, *128*, 9394−9407.
(38) Rausch, D.; Lambert, C. *Org. Lett.* **2006**, *8*, 5037−5040.
(39) Liddell, P. A.; Kodis, G.; de la Garza, L.; Moore, A. L.; Moore, T. A.; Gust, D. *J. Phys. Chem. B* **2004**, *108*, 10256−10265.
(40) Cho, H. S.; Rhee, H.; Song, J. K.; Min, C. K.; Takase, M.; Aratani, N.; Cho, S.; Osuka, A.; Joo, T.; Kim, D. *J. Am. Chem. Soc.* **2003**, *125*, 5849−5860.
(41) Kodis, G.; Terazono, Y.; Liddell, P. A.; Andreasson, J.; Garg, V.; Hambourger, M.; Moore, T. A.; Moore, A. L.; Gust, D. *J. Am. Chem. Soc.* **2006**, *128*, 1818−1827.
(42) Keirstead, A. E.; Bridgewater, J. W.; Terazono, Y.; Kodis, G.; Straight, S.; Liddell, P. A.; Moore, A. L.; Moore, T. A.; Gust, D. *J. Am. Chem. Soc.* **2010**, *132*, 6588−6595.
(43) Chebny, V. J.; Shukla, R.; Rathore, R. *J. Phys. Chem. A* **2006**, *110*, 13003−13006.
(44) Chebny, V. J.; Dhar, D.; Lindeman, S. V.; Rathore, R. *Org. Lett.* **2006**, *8*, 5041−5044.
(45) Jimenez-Garcia, L.; Kaltbeitzel, A.; Enkelmann, V.; Gutmann, J. S.; Klapper, M.; Müllen, K. *Adv. Funct. Mater.* **2011**, *21*, 2216−2224.
(46) Zhi, L.; Müllen, K. *J. Mater. Chem.* **2008**, *18*, 1472−1484.
(47) Schore, N. E. *Chem. Rev.* **1988**, *88*, 1081−1119.
(48) Steeger, M.; Lambert, C. *Chem.—Eur. J.* **2012**, accepted for publication.
(49) Thiebes, C.; Prakash, G. K. S.; Petasis, N. A.; Olah, G. A. *Synlett* **1998**, 141−142.
(50) Angulo, G.; Grarapp, G.; Rosspeintner, A. *Spectrochim. Acta A* **2006**, *65*, 727−731.
(51) Strickler, S. J.; Berg, R. A. *J. Chem. Phys.* **1962**, *37*, 814−822.
(52) Heckmann, A.; Lambert, C. *J. Am. Chem. Soc.* **2007**, *129*, 5515−5527.
(53) Kaupp, M.; Renz, M.; Parthey, M.; Stolte, M.; Würthner, F.; Lambert, C. *Phys. Chem. Chem. Phys.* **2011**, *13*, 16973−16986.
(54) Stahl, R.; Lambert, C.; Kaiser, C.; Wortmann, R.; Jakober, R. *Chem.—Eur. J.* **2006**, *12*, 2358−2370.
(55) Dorfman, R. C.; Lin, Y.; Fayer, M. D. *J. Phys. Chem.* **1989**, *93*, 6388−6396.
(56) Lakowicz, J. R. *Principles of Fluorescence Spectroscopy*, 3rd ed.; Springer: Berlin, 2006.
(57) Hall, R. D.; Valeur, B.; Weber, G. *Chem. Phys. Lett.* **1985**, *116*, 202−205.
(58) Dörr, F. *Angew. Chem., Int. Ed.* **1966**, *78*, 457−474.
(59) Verbouwe, W.; Auweraer, M. V. d.; Schryver, F. C. D.; Piet, J. J.; Warman, J. M. *J. Am. Chem. Soc.* **1998**, *120*, 1319−1324.
(60) Demidov, A. A.; Andrews, D. L. *Photochem. Photobiol.* **1996**, *63*, 39−52.
(61) Valeur, B.; Weber, G. *J. Chem. Phys.* **1978**, *69*, 2393−2400.
(62) Leroy, E.; Lami, H. *Chem. Phys. Lett.* **1976**, *41*, 373−377.
(63) Kasha, M.; Rawls, H. R.; El-Bayoumi; Ashraf, M. *Pure Appl. Chem.* **1965**, *11*, 371−392.
(64) The interaction matrix for this case is analogous to the Hückel-π-MO-matrix for benzene in which the resonance integral has to be replaced by the exciton interaction *V*.
(65) Vauthey, E. *ChemPhysChem* **2012**, *13*, 2001−2011.
(66) Piet, J. J.; Biemans, H. A. M.; Warman, J. M.; Meijer, E. W. *Chem. Phys. Lett.* **1998**, *289*, 13−18.

(67) Melhuish, W. H. *J. Phys. Chem.* **1961**, *65*, 229−235.
(68) Thompson, A. L. S.; Kabalka, G. W.; Akula, M. R.; Huffman, J. W. *Synthesis* **2005**, 547−550.
(69) Lambert, C.; Nöll, G.; Schmälzlin, E.; Meerholz, K.; Bräuchle, C. *Chem.—Eur. J.* **1998**, *4*, 2129−2135.